A Monte Carlo Study on a 3-Dimensional Comb Polymer Translocation through a Nanopore driven by an Electric Field

MSc Thesis submitted to

The Department of Physics

College of Natural & Computational Science

Addis Ababa University

by

Bruh Tesfa Bedassa

Advisor:

Dr. Tatek Yergou (Associate Professor of Physics)

January, 2024 Addis Ababa, Ethiopia

Addis Ababa University

College of Natural Sciences

School of Graduate Studies

This is to certify that the thesis prepared by Bruh Tesfa, entitled: *A Monte Carlo Study on a 3-Dimensional Comb Polymer Translocation through a Nanopore driven by an Electric Field* and submitted in partial fulfillment of the requirements for the Degree of Master of Science in Statistical Physics, complies with the regulations of the university and meets the accepted standards with respect to originality and quality.

Approved by:

Advisor

Dr. Tatek Yergou	Signature	Date .....

Examiners

1. Dr. Mulugeta Bekele	Signature	Date .....
2. Dr. Lemi Demeyu	Signature	Date .....

Department Head

Prof. Fekadu Gashaw	Signature	Date .....

Abstract

A lattice Monte Carlo study of comb polymers translocation through a nanopore subject to an electric field is presented. Our approach is universal in a sense that we are not limited to single file translocations. Instead, we investigated single file translocations as a particular case in this universal approach. In this way, we have made an extensive study on the translocation dynamics of comb polymers as a function of field strength, pore size, and the comb polymer's topology. We were able to show the existence of a critical field strength for any particular system. The difference between the most probable translocation time and the mean translocation time is minimum at the critical field strength. Also, the critical field strength helped us to identify two regimes of translocations with different properties. We named them as smooth and chaotic translocations. These results should also be valid for linear polymers because linear polymers are comb polymers without side chains. In addition, we took advantage of the side chains of comb polymers to study the pore-polymer interaction in an unprecedented way by varying the side chain lengths. This enabled us explain the varied values of α in $\langle\tau\rangle \sim N^{\alpha}$, where $\langle\tau\rangle$ is the mean translocation time and N is the chain length of a linear polymer, in the literature.

Acknowledgment

This research has been a tough journey for me. From the first idea to the simulation code development and test, and then to the analysis of the generated data and the final writing of the findings, I had help from many individuals. But, first, I would like to acknowledge and thank God for this final accomplishment.

"Many are the plans in a man's heart, but it is the Lord's purpose that prevails." (Proverbs 19:21, NIV)

My family sponsored me. They take the lion's share of my gratitude. Next, I would like to say thank you to all MSc and PhD students with whom I shared the statistical physics computer laboratory in our department. They have allowed me to use their computers for the generation of the large amount of data required for studying the research problem. It would have been impossible for me to finish the research in time without their cooperation and understanding as the simulation required a high computational power. Their names are Shinie, Husen, Begashaw, Derese, Meseret, Emru, Abebe, and Dagne. I want to separate out one man from these names: Shinie Shewangzaw. He has been of a tremendous help in many respects which I cannot list all here. In addition to his exceptional academic achievements, he is a very kind and humble person.

Analysis of a large data is not a picnic without the right tools. In this regard, Henok Fekade, a software engineering graduate and my cousin, helped me by introducing me to the Python programming language. He also helped me in writing vital Python codes that I used for managing the data files.

Contents

List of Figures

List of Tables

Chapter 1

Introduction

A polymer is a set of small repeating molecules joined together by a covalent bond resulting in a new molecule with unique properties. The repeating molecules are known as monomers. A given polymer may have several unique monomers. If it has just one kind of monomer, it is called homopolymer; otherwise, we call it a heteropolymer. The properties of a polymer is as determined by the chemical identity of its monomers as the way its constituting monomers are connected together. The way with which monomers form a polymer could mean: (a) the sequence of the monomers (in heteropolymers) (b) the way the atoms of the monomers are arranged in a polymer (called the polymer's microstructure) (c) the way the segments of the polymer are connected to one another (called the polymer architecture) [1]. There are several types of polymer architecture. But, the types discussed in this thesis are the linear polymer and the comb polymer (see figure 1.1).

The number of monomers in the polymer, called the degree of polymerization, also plays its own role in the properties of a polymer. The degree of polymerization of a polymer can reach a billion. This invites the use of the tools of statistical mechanics

(a) Linear Polymer

(b) Comb Polymer

Figure 1.1: Two architectures of a polymer.

for the analysis of such macromolecule in terms of its constituent monomers and the interactions among them. In the subsequent sections, we will take a glimpse of this method and gain some insight into the characterstics of an isolated polymer.

1.1 The ideal chain

1.1.1 The random-walk model

We begin our theoretical study on polymers in a very simple manner where we assume that the polymer chain follows a regular lattice. The portions of the polymer lying on the lattice points are called 'segments', and the rods connecting the segments are called 'bonds'. Let b be the length of each bond and z the coordination number of the lattice. In our ideal model, each segment can make a bond with its neighbour along any direction and each direction is equally likely. The pattern of all the bonds thus formed is then exactly identical to the path followed by a random walker on the lattice.

From the theory of random-walks, the probability density of a three-dimensional random walker at position $\mathbf{R}$ after a total of N steps taken from the origin is given by

$$P(\mathbf{R}, N) = \left(\frac{3}{2\pi N b^2}\right)^{\frac{3}{2}} \exp\left(-\frac{3\mathbf{R}^2}{2Nb^2}\right). \tag{1.1}$$

for large N [2]. For the problem at hand, $P(\mathbf{R}, N)\, dR$ represents the probability that a long polymer has the end-to-end vector $\mathbf{R}$.

Clearly, the average value $\langle \mathbf{R} \rangle$ of $\mathbf{R}$ is zero (because the probability of the end to end vector being $\mathbf{R}$ is the same as it being $-\mathbf{R}$ so that the two contributions cancel out). Therefore, we will calculate $\langle \mathbf{R}^2 \rangle$:

$$\langle \mathbf{R}^2 \rangle = \sum_{n=1}^{N} \sum_{m=1}^{N} \langle \mathbf{r}_n \cdot \mathbf{r}_m \rangle,$$

where $\mathbf{r}_n$ is the vector of the n^{th} bond. If $n \neq m$, $\langle \mathbf{r}_n \cdot \mathbf{r}_m \rangle = \langle \mathbf{r}_n \rangle \cdot \langle \mathbf{r}_m \rangle = 0$. So,

$$\langle \mathbf{R}^2 \rangle = \sum_{n=1}^{N} \langle {\mathbf{r}_n}^2 \rangle = Nb^2$$

That is, the size of the polymer is proportional to $N^{\frac{1}{2}}$.

1.1.2 The effect of short-range interactions

In the preceding model, we assumed that the orientations of each bond is random and this means that the polymer is able to fold back onto itself at certain locations which is a physical impossibility since two portions of the polymer cannot occupy the same region in space. To remedy this, let us agree that the bond vector $\mathbf{r}_{n+1}$ is not allowed to point back to the previous step, i.e., it cannot take the direction $-\mathbf{r}_n$. Thus, in this model, the average value of $\mathbf{r}_{n+1}$ will not be zero for a given $\mathbf{r}_n$. Writing this average as $\langle \mathbf{r}_{n+1} \rangle_{\mathbf{r}_n}$, it is clear that

$$0 = \sum_{i=1}^{z} \mathbf{b}_i = (z-1)\langle \mathbf{r}_{n+1} \rangle_{\mathbf{r}_n} - \mathbf{r}_n,$$

where $\mathbf{b}_i (i = 1, ..., z)$ stands for all the bond vectors the polymer can take. Consequently, $\langle \mathbf{r}_{n+1} \rangle_{\mathbf{r}_n} = \dfrac{1}{z-1}\mathbf{r}_n$ so that

$$\langle \mathbf{r}_{n+1} \cdot \mathbf{r}_n \rangle = \frac{b^2}{z-1}.$$

In the same way, we can calculate $\langle \mathbf{r}_{n+2} \cdot \mathbf{r}_n \rangle$:

$$\langle \mathbf{r}_{n+2} \cdot \mathbf{r}_n \rangle = \langle \langle \mathbf{r}_{n+2} \rangle_{\mathbf{r}_{n+1}} \cdot \mathbf{r}_n \rangle = \frac{1}{z-1}\langle \mathbf{r}_{n+1} \cdot \mathbf{r}_n \rangle = \frac{b^2}{(z-1)^2}$$

So, in general,

$$\langle \mathbf{r}_n \cdot \mathbf{r}_m \rangle = \frac{b^2}{(z-1)^{|n-m|}}$$

and $\langle \mathbf{R}^2 \rangle$ becomes

$$\langle \mathbf{R}^2 \rangle = \sum_{n=1}^{N}\sum_{m=1}^{N}\langle \mathbf{r}_n \cdot \mathbf{r}_m \rangle = \sum_{n=1}^{N} \underline{\sum_{k=-n+1}^{N-n} \frac{b^2}{(z-1)^{|k|}}}$$

If N is very large, then, for almost all n, the underlined summation can be replaced by one for k from $-\infty$ to ∞, giving

$$\langle \mathbf{R}^2 \rangle = \sum_{n=1}^{N}\sum_{m=1}^{N}\langle \mathbf{r}_n \cdot \mathbf{r}_m \rangle = \sum_{n=1}^{N}\sum_{k=-\infty}^{\infty} \frac{b^2}{(z-1)^{|k|}} = Nb^2\frac{z}{z-2}$$

Therefore, even with our modified model of the polymer, there is no change in the fundamental result that $\langle \mathbf{R}^2 \rangle$ is proportional to N for large N.

In general, if the interaction between the bonds extends only up to a finite distance along the chain, then the quantity $\langle \mathbf{r}_n \cdot \mathbf{r}_m \rangle$ will decay exponentially for large $|n-m|$.

For such systems $\langle \mathbf{R}^2 \rangle$ is always proportinal to N for large N, and the distribution of $\mathbf{R}$ is Gaussian. In this sense, polymer models with local bond interactions are equivalent to random walk model, and such polymer chains are called 'ideal chains'. The average of the square of the end-to-end distance of an ideal chain can be written

$$\langle \mathbf{R}^2 \rangle = N {b_{eff}}^2,$$

where b_{eff} is called the effective bond length. From now on, for simplilcity, we will write b for b_{eff}.

1.1.3 Radius of gyration of an ideal chain

The radius of gyration R_g of a polymer is defined as

$${R_g}^2 = \frac{1}{2N^2} \sum_{n=1}^{N} \sum_{m=1}^{N} \langle (\mathbf{R}_n - \mathbf{R}_m)^2 \rangle$$

where $\mathbf{R}_n$ is the position vector of the n$^{\text{th}}$ segment. It happens that the radius of gyration R_g is a more convenient way of expressing the size of a polymer than the average of the square of the end-to-end vector $\langle \mathbf{R}^2 \rangle$. The radius of gyration can be directly measured in experiments and can also be defined not only for linear polymers but also for polymers with branched structure, etc.

1.2 Non-ideal chains

1.2.1 The excluded volume effect

The ideal chain model only takes into account the short range interactions. Thus, this model permits a chain to loop back onto itself so that segments which are widely separated along the chain will occupy the same region in space. Of course, this is a physical impossibility. If we model the polymer as a connected path on a lattice, this effect can be accounted for by imposing the condition that the path cannot pass through any sites that have been traversed previously. This is called a 'self-avoiding walk' and the polymer thus represented is called an 'excluded volume chain'.

Obiviously, the average size of an excluded volume chain is larger than that of an ideal chain as overlapping of segments is forbidden in the former one. Let us now estimate

this effect by a simple model. Consider the quantity $W(R)dR$ which is the total number of excluded volume chains with the N^{th} step lying at a distance between R and $R+dR$ from the origin. In order to calculate $W(R)dR$, let us first ignore the excluded volume effect and calculate the total number of ideal chains $W_0(R)dR$. The overall number of ideal chains with N steps is z^N and the probability of the distance being between R and $R+dR$ is $P(\mathbf{R}, N)4\pi R^2\, dR$, using the probability distribution function of Equation 1.1. So,

$$W_0(R) = z^N 4\pi R^2 \left(\frac{3}{2\pi N b^2}\right)^{\frac{3}{2}} \exp\left(-\frac{3R^2}{2Nb^2}\right)$$

Let $p(R)$ be the probability that an ideal chain configuration is also allowable under the excluded volume condition. To estimate $p(R)$, assume that the polymer segments are evenly distributed in a region of volume R^3. If we write the volume of one lattice element as ν_c, there will be $\frac{R^3}{\nu_c}$ lattice sites in the volume. We now calculate the probability that no overlaps occur when we place N segments on these lattice sites. The probability that one particular segment will not overlap with another is given by $(1-\frac{\nu_c}{R^3})$. Since there are $N(N-1)/2$ possible combinations of segment pairs, the probability that no overlap occurs in all of these combinations is given by

$$p(R) = (1-\frac{\nu_c}{R^3})^{N(N-1)/2} = \exp\left(\ln(1-\frac{\nu_c}{R^3})\frac{1}{2}N(N-1)\right).$$

Since $R^3 \gg \nu_c$, $\ln(1-\frac{\nu_c}{R^3}) \approx \frac{\nu_c}{R^3}$. Assuming $N \gg 1$, we obtain

$$p(R) = \exp\left(\frac{-N^2\nu_c}{2R^3}\right).$$

Therefore,

$$W(R) = W_0(R)p(R) \propto R^2 \exp\left(\frac{-3R^2}{2Nb^2} - \frac{N^2\nu_c}{2R^3}\right).$$

Both $W_0(R)$ and $W(R)$ have a maximum at certain values of R. Let us estimate the average size of the polymer chain in each model by calculating the positions of these maxima. The maximum of $W_0(R)$ occurs at $\tilde{R_0} = \left(\frac{2Nb^2}{3}\right)^{1/2}$. The maximum of $W(R)$ occurst at $\tilde{R}$, which satisfies the following equation obtained by differentiating the logarithm of $W(R)$:

$$\frac{-3\tilde{R}^2}{2Nb^2} + \frac{3N^2\nu_c}{4\tilde{R}^3} + 1 = 0.$$

Combining these, we obtain

$$\left(\frac{\tilde{R}}{\tilde{R_0}}\right)^5 - \left(\frac{\tilde{R}}{\tilde{R_0}}\right)^3 = \frac{9\sqrt{6}\nu_c\sqrt{N}}{16b^3}.$$

If $N \gg 1$, the second term on the left-hand side can be neglected so that

$$\tilde{R} \approx \tilde{R}_0 \left(\frac{N^{1/2} \nu_c}{b^3} \right)^{1/5} \propto N^{3/5}.$$

We see that the characteristic size of excluded volume chains is proportional to $N^{3/5}$, and not $N^{1/2}$. The above is very rough theory of the excluded volume effect. The statistical properties of excluded volume chains have been extensively investigated in numerical simulations, and for large N, it has been found that the size obeys the following formula:

$$R_g \propto N^{\nu} b$$

where the exponent ν is approximately 0.588, very close to the value $\frac{3}{5}$ calculated above [2].

1.3 Objective and Method

This thesis is devoted to a numerical study of an electric field driven 3D translocation of comb polymers. Comb polymers are polymers having a long main chain, referred to as the backbone, with numerous side chains extending from it. These side chains are typically short and are attached regularly along the backbone, resembling the teeth of a comb. While the translocation process of linear polymers has been vigorously studied, the translocation of other polymer architectures are barely explored. To our best knowledge, no published experimental study has been made on the translocation of comb polymers to this day. Even simulation studies on comb polymers are hard to find (if not non-existent) in the literature. We hope that this numerical study will help fill this gap.

Our preferred method of study is the Monte Carlo (MC) simulation technique using the fluctuating bond (FB) [46] model of a polymer. The FB model is an excellent model for non-ideal chains (see section 1.2) while the MC algorithm allows one to study the dynamics of a system by simulation in accordance with the principles of statistical mechanics.

Oh what a bottle-neck has it been for me! But now, I have finally translocated.

Chapter 2

Literature Review

Imagine a polymer suspended in some kind of a solvent. The solvent is in a two-compartment chamber and we name the compartments as the *cis* side and the *trans* side. Our polymer is inside the *cis* side. Let us make a small hole (relative to the size of the polymer) on the wall separating the two compartments. Now, there is a possibility for the polymer to move to the *trans* side of the chamber if the size of the hole is at least as large as the monomers of the polymer.

If the polymer is to get to the *trans* side, it has to first come to where the hole is located and then undergo a process called 'translocation' to cross the wall. The process begins with the movement of some monomers into the hole. Because of the connectivity of the monomers, this calls for a similar movement of the adjacent monomers in the bond chain. In this way, the polymer as a whole starts getting squeezed into the hole. As the process continues, the first monomers to get into the hole come out of it on the other side of the wall. As they move deeper and deeper into the *trans* side compartment, more and more monomers emerge from the hole. The emergence of the last monomers in the bond chain out of the hole signals the end of the translocation process.

However, the occurrence of translocation with a mere thermally-induced movement is extremely unlikely. This is because the polymer will be forced to lose a significant number of its conformational states if it is to move through the pore [3]. There are a variety of techniques that are employed to overcome this entropic barrier. One of them is setting up an electrical potential difference between the two compartments. For this to work, of course, the polymer should be charged in the first place.

In an experiment, a salt is also added into the solvent. This is necessary for observing the translocation process in terms of the ion current that builds up when a potential difference is set up between the two compartments. If the solution in the chamber is free from any kind of polymer, an ion current of fixed magnitude can be measured at the hole. But, if the solution is polymer infested, this ion current will decrease whenever a polymer comes close to the hole and interferes with the flow of the ions through the hole. This decrement in the ion current will be even worse if the polymer starts translocating through the hole as this would result in a blockage of the hole. When the polymer is finally out of the hole, the ion current jumps back to its previous value. Thus, the real-time reading of the ion current at the hole gives us a way of observing the polymer translocation phenomenon.

We can take this idea even farther for a linear polymer. Since translocation of a polymer essentially involves the straightening out of the polymer so that it can get through the hole, we can get the polymer completely straightened out by making the hole small enough. Such kind of translocation process where no folded segments of the polymer can fit inside the hole is known as a single file translocation. If the hole is also short enough so that only one monomer can be inside the hole at a time, then the ion-current reading during the time of translocation should register the entrance and exit of each monomer. This ion-current reading of a translocating polymer at a single monomer resolution could in principle be used to differentiate between different kinds of monomers that may be lying at different positions along the polymer chain. In other words, we can obtain the sequence of the monomers in the polymer chain in the order from one end of the chain to the other one by appropriately analyzing such ion-current reading. In particular, we can use this technique to sequence DNA and this is one of the chief motivating factors in the efforts made to understand the translocation phenomenon [4].

The polymer translocation (PT) idea explained in the above paragraphs was almost entirely contained in the pioneering paper by Kasianowicz *et al.* published in 1996 [5]. This exciting publication led to numerous theoretical [6–15], experimental [16–25] and numerical [26–36] efforts to understand the PT phenomenon that continues to this day. The work by Kasianowicz *et al.* was experimental where homopolymer RNA molecules (mainly polyuridylic acid) are made to undertake a single file translocation through a biological pore (specifically, the α-hemolysin pore) embedded in a lipid bilayer parti-

tioning a buffer-filled chamber into two. Both sides of the chamber contained a solution of 1 M KCl and the translocation was driven by an electric field. By analyzing the histogram of current blockage lifetime, they found that the mean lifetime is proportional to the homopolymers length N. This marked the discovery of a new method for the characterization of macromolecules.

The biological pore α-hemolysin has a nonuniform width which measures ∼1.4 nm at its narrowest part [37]. This is just enough to accommodate a single-stranded DNA molecule. The pore has been the choice protein pore in translocation experiments for its relative stability among other things [38, 39].

In 2001, Li *et al.* produced the first artificial nanopores in silicon-nitride membranes using a technique they called an ion-beam sculpting [40]. The pore produced this way could be as narrow as 1.8 nm. In 2003, Storm *et al.* discovered another way for fabricating artificial nanopores [41]. They used silicon-oxide membranes and were able to produce nanopores with a width of 1 nm. Unlike their biological counterparts, the width of these solid-state nanopores is tunable. Also, solid-state nanopores have the advantage of being significantly more stable than bio-pores to environmental changes in temperature, pH, *etc.* [38, 39].

Soon, experiments on PT employing these solid-state nanopores started being performed. In 2004, Chen *et al.* used an ion beam sculpted nanopore to perform a translocation experiment on double-stranded DNA molecules [22]. The nanopore they used has a diameter of ∼15 nm. Since the cross-section of a double-stranded DNA molecule is about 2.4 nm, the molecule can translocate through the pore not only as an extended molecule but also in a folded configuration [18]. It is obvious that higher current blockage results when the molecule translocates in a folded configuration rather than in a single file manner. Chen *et al.* made advantage of this to isolate the cases of only single file translocations. Their findings indicated a linear relationship between mean PT time and the chain length of the DNA, just as in the translocation experiments with α-hemolysin pore.

In 2005, Storm *et al.* performed another translocation experiment on double-stranded DNA molecule using a differently fabricated solid-state nanopore [20]. This time the diameter of the nanopore was ∼10 nm. Like Chen *et al.*, Storm *et al.* filtered out the single-file translocation cases for analysis. Unlike any time before, they arrived at the

conclusion that the mean PT time and the chain length N of the DNA molecule did not follow a linear relationship. Instead, they reported a power-law relationship between the two variables: $\langle \tau \rangle = N^{1.30}$.

These differences in the scaling properties of PT through a solid-state nanopore have not been adequately explained so far. Also, the fast and cheap sequencing of DNA people hoped to achieve by the PT method [42, 43] is still out of reach although people have been working on it since 1996. The full understanding of the dynamics of polymers has proven to be quite challenging and non-trivial [44], and such an understanding would certainly help the realization of some PT applications like DNA sequencing [45]. Maybe, it is time to change our approach of attacking the problem to meet this challenge.

It is interesting that linear polymers can be viewed as comb polymers with no side chains. Therefore, in principle, their translocation through a nanopore can be studied within the framework of the study of the translocation of comb polymers. This approach of studying the translocation of linear polymers might shade light on some of the poorly understood properties of linear PT observed in various experiments performed so far, either in the long run or immediately here. We will give some examples on this matter as we go along.

In this thesis, we will try to map the roles of various major actors in the translocation phenomenon including the effects of the field strength, pore radius, and chain size, in terms of side chain length and backbone length, of the comb polymer. As a measure of the PT dynamics, we use the PT time τ as our major quantity. The PT time is the time it takes for the polymer to move from the *cis* side to the *trans* side through the nanopore. We basically try to find the relationship between the above-mentioned various factors affecting the PT phenomena and the PT time. In doing so, we discover several interesting features of the translocation phenomena and many of them also apply to linear polymers. In our study, we will not be limited to the single file translocation of comb polymers but we will give a special attention to it and discuss it under various scenarios every now and then.

Chapter 3

Methodology

This study is performed by a computer simulation. The physical problem is simulated via the MC method in combination with the FB model of a polymer. The FB model [46] is a lattice model of a polymer that mimics the behavior of a real polymer by allowing the bond lengths between the monomers of the polymer to fluctuate. In three dimensions, the bond length between any two monomers has to be within the interval $[2, \sqrt{10}]$ in this model. The lower limit of the bond length is set in order to avoid volume overlapping of the bonded monomers. The upper limit is to make sure that there are no bond cuts.

3.1 Simulation details

The comb polymer is constructed in such a way that side chains of length N_S are grafted onto every monomer of the backbone (which is of length N_B), except the end monomers. It is then placed at the center of a large box of length at least $8N_B$ and width/height $\geq 4N_B$ for equilibration. The equilibration is carried out by randomly selecting a monomer from the comb polymer and moving it to one of the adjacent lattice sites in a randomly selected direction. If the new lattice site is already occupied by another monomer or is very close to it (by less than 2 lattice units), the move is undone. The move is also undone if it causes the distance between the monomer and any of its neighboring monomers bonded to it to be outside the interval $[2, \sqrt{10}]$, in accordance with the FB model. Whether the new lattice site is accepted or rejected, another move attempt with another randomly chosen monomer is performed. This process is repeated

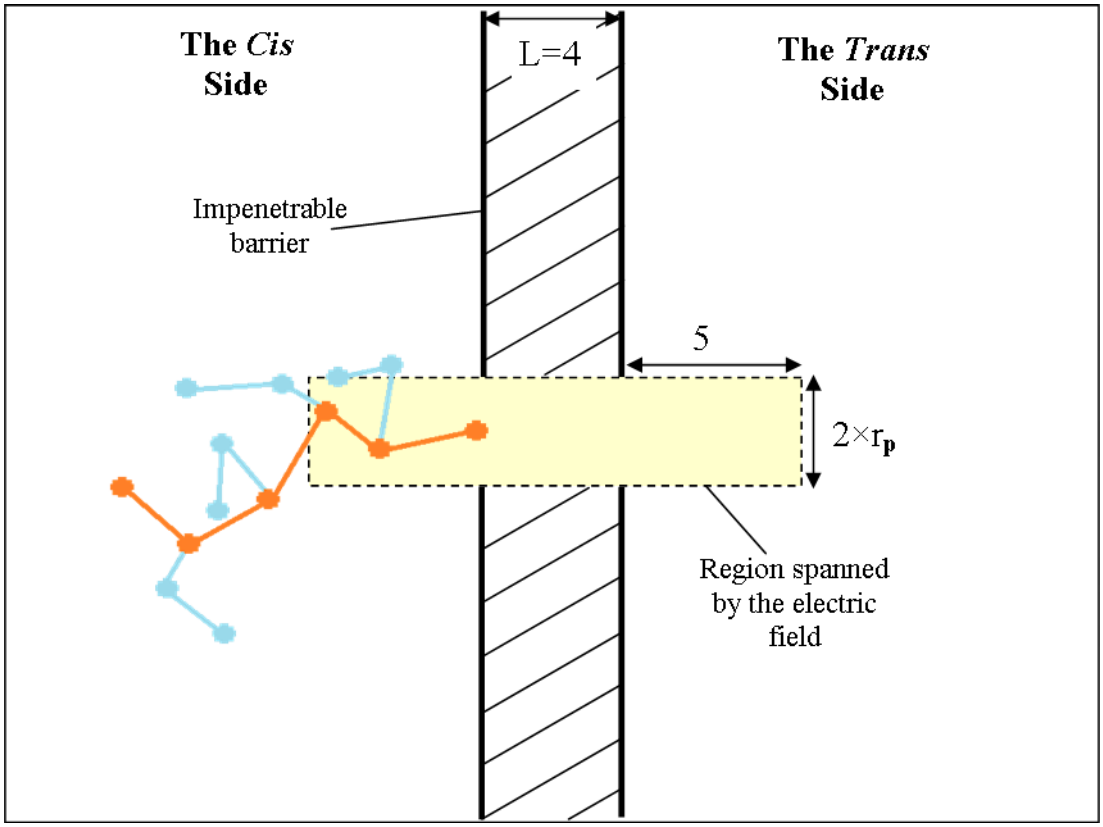

Figure 3.1: Lateral view of the simulation layout for the translocation process

over and over again until one million move attempts are made for each monomer of the comb polymer on average.

The membrane separating the *cis* side from the *trans* side is constructed from a single sheet of immovable monomers. This makes the membrane four lattice units thick as shown in figure 3.1. A pore is made at the center of the membrane by removing the monomers at the center of the membrane. The removal is done in such a way that the pore formed is square-shaped of side $2r_p$.

The external force employed to drive the PT is similar to the one used by Chern *et al.* [29]. The only difference is that the one used here protrudes from the pore on both sides by five lattice units (see figure 3.1). This alteration is made in an attempt to reduce the fraction of polymers that retract from the pore. The external force acts by virtue of an electrical potential difference existing between different lattice sites. The potential U_e

profile in a coordinate system centered at the center of the pore is described as follows:

$$U_e(x,y,z) = \begin{cases} -xE & \text{if } \frac{L}{2}+5 \geq x \geq -\frac{L}{2}-5, \\ & \quad |y| \leq r_p, \text{ and } |z| \leq r_p; \\ -(\frac{L}{2}+5)E & \text{if } x > \frac{L}{2}+5; \\ (\frac{L}{2}+5)E & \text{if } x < -\frac{L}{2}-5; \text{ and} \\ \infty & \text{otherwise,} \end{cases}$$

where $L = 4$ is the depth of the pore, E is the electric field strength, and r_p is the pore radius (which is half of the width of the pore). This potential difference profile creates a uniform electric field directed towards the *trans* side. In this simulation, every monomer of the comb polymer is affected by the electric field as if each monomer has a unit positive electric charge.

3.2 The translocation process

Once the comb polymer has reached its equilibrium state, it undergoes a parallel translation so that the rightmost monomer is at the entrance of the pore as shown in figure 3.2. The translocation process is then launched with a first move attempt of a randomly selected monomer of the comb polymer. The success or failure of the move attempts in the translocation process is governed by the same rules as in the equilibration process but with one more addition. Here, the energy of the old and new states of the monomer is also taken into account. Explicitly, a move attempt is successful only within a probability of $\min[e^{-\Delta U/k_BT}, 1]$, where ΔU is the change in the energy from the old state to the new state, k_B is the Boltzmann's constant, T is temperature, even if it fulfills all the other criteria. Incidentally, we note that we will use $\delta\epsilon = \dfrac{E}{k_BT}$ as an electric field strength instead of just E because we do not deal with the effect of temperature variations on the PT in this thesis.

The polymer is given a total of 250 million move attempts to get to the *trans* side of the membrane. If it cannot do this after all these move attempts, the polymer is considered as stuck and the translocation process is aborted. Also, if the polymer retracts away from the pore so that the rightmost monomer of the polymer is four lattice units away from the pore entrance, the translocation process is aborted. However, if the translo-

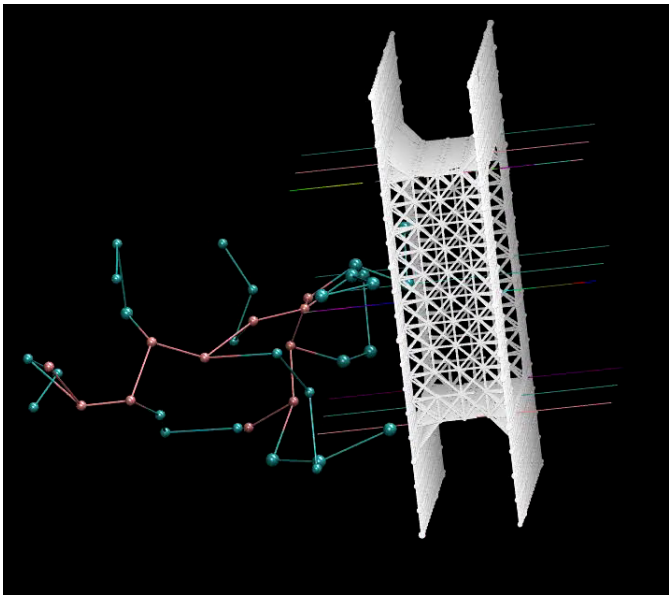

Figure 3.2: A VMD (Virtual Molecular Dynamics) software generated visualization of a relaxed comb polymer ($N_B = 11, N_S = 3$) at the entrance of a pore ($r_p = 5$) just before a translocation process. The red colored chain of the comb polymer is the backbone while the blue colored chains are the side chains. The white colored object is the membrane with the pore embedded on it. The thin, colored lines represent electric field lines.

cation process is completed within the maximum number of move attempts, the total number of move attempts made by all monomers of the polymer divided by the total number of the monomers is taken as the MC time of translocation τ of the polymer. Since the values of τ tend to be distractingly high, we rescaled them by a factor of 10^{-3}.

The above procedure of a translocation trial from equilibration of the comb polymer to a translocation process is repeated over and over again until thousands of successful translocation trials are attained.

Chapter 4

Results and Discussion

4.1 The dependence of the PT time τ on the electric field strength $\delta\epsilon$

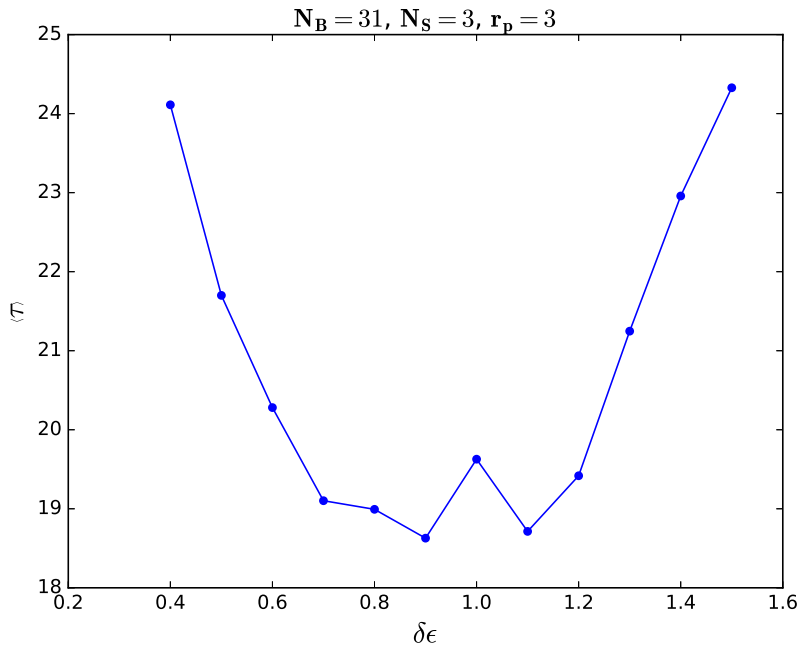

Figure 4.1: Dependence of the mean PT time $\langle\tau\rangle$ on the field strength $\delta\epsilon$

Examination of the behavior of the translocation dynamics as a function of the electric field strength was undertaken for comb polymers with backbone length as long as $N_B = 61$. As a preliminary result, we find that the mean PT time has a non-monotonic relationship with the electric field strength as shown in figure 4.1. To gain more insight

into this behavior, we studied how the distribution of the PT time is affected when the electric field strength varies (see table 4.1). As the field strength increases, the distribution of the PT time contracts steadily, mainly from the right side, until the field strength reaches a certain value $\delta\epsilon_c$, which is unique to the pore size if all the other variables of translocation are held constant. In other words, the tail of the PT time distribution curve gets shorter and shorter as the electric field strength increases to $\delta\epsilon_c$. We call $\delta\epsilon_c$ the critical field strength. Beyond the critical field strength, the distribution starts to spread out – with some fluctuation at first. As for the mean PT time, it decreases steadily as the field strength increases to $\delta\epsilon_c$ reflecting the narrowing down of the PT time distribution. Then, it fluctuates until it starts to increase steadily.

Table 4.1: Tabular representation of the PT time distributions of a comb polymer with ($N_B = 31$, $N_S = 3$) translocating through a pore of size $r_p = 3$ under various field strengths. The distributions are prepared from a dataset of 4500 data points.

	Intervals of the PT time						Field Strength
	$\tau \leq 50$	$(50, 100]$	$(100, 150]$	(150,200]	$(200, 250]$	$\tau > 250$	
Frequency	4444	48	6	1	1	0	**0.4**
	4475	19	4	2	0	0	**0.5**
	4493	7	0	0	0	0	**0.6**
	4499	1	0	0	0	0	**0.7**
	4494	5	1	0	0	0	**0.8**
	4493	4	1	1	0	1	**0.9**
	4483	4	3	2	1	7	**1.0**
	4484	7	2	0	1	6	**1.1**
	4460	16	10	5	0	9	**1.2**
	4443	20	13	1	2	21	**1.3**
	4410	30	18	9	3	30	**1.4**
	4398	36	20	11	8	27	**1.5**

This behavior of the field strength dependence of the PT time can also be studied as

a function of the pore size. Figure 4.2 reveals a counterintuitive trend as the pore size decreases from $r_p = 2$ to $r_p = 1$. It is natural to expect the fraction of stuck polymers to decrease as the pore size increases and this is true for all pore sizes except pore size $r_p = 1.5$. The pore $r_p = 1.5$ has hosted a larger number of stuck cases than the pore $r_p = 1$ for translocation simulations with $\delta\epsilon \geq 0.5$.

However, we need to quickly note that the critical field strength for the pore $r_p = 1.5$ is 0.4. For the pore size $r_p = 1$, $\delta\epsilon_c$=0.5 while $\delta\epsilon_c$=0.8 for $r_p = 2$. If we now look at figure 4.2 more closely, we see that the change in the fraction of the stuck cases for each pore size as the field strength increases to $\delta\epsilon_c$ is negligible. For $\delta\epsilon \geq \delta\epsilon_c$, however, the fraction of stuck cases for each pore size start to rapidly increase as the field strength increases. This increase is more serious for the pore size $r_p = 1.5$ than the other two pore sizes. Thus, it happens that PT through a pore of size $r_p = 1.5$ is very sensitive to the field strength.

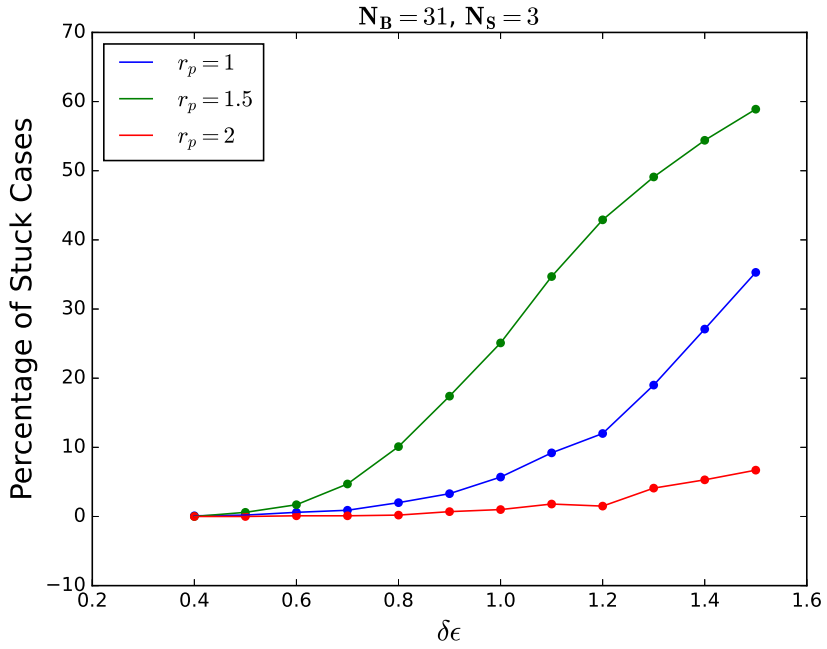

Figure 4.2: Dependence of the fraction of stuck comb polymers on the field strength for various pore sizes

We note that the narrower the pore is, the more likely is a single file translocation. We also note that only a single file translocation is possible with the pore size $r_p = 1$. It then follows that PT through a pore of size $r_p = 1.5$ is a transition from a regime of translocation where polymers can translocate as folded configuration to the one where

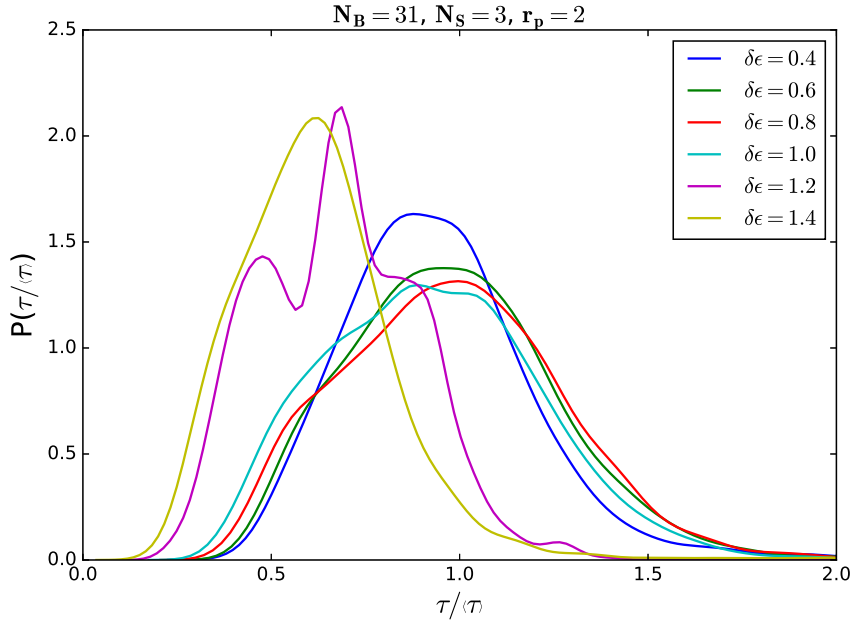

(a) $r_p = 2$

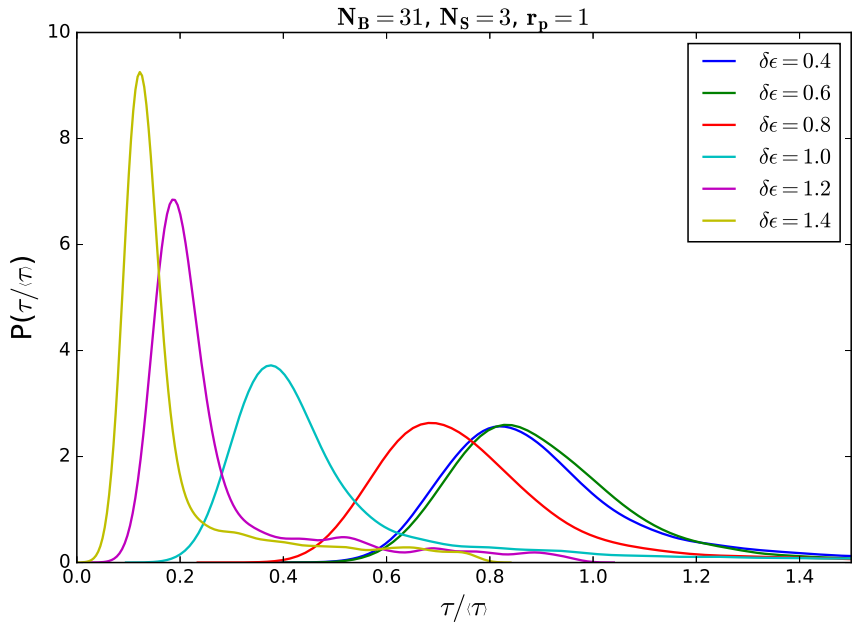

(b) $r_p = 1$

Figure 4.3: Normalized distribution graphs of $\tau/\langle\tau\rangle$ for two pore sizes $r_p = 2$ and $r_p = 1$

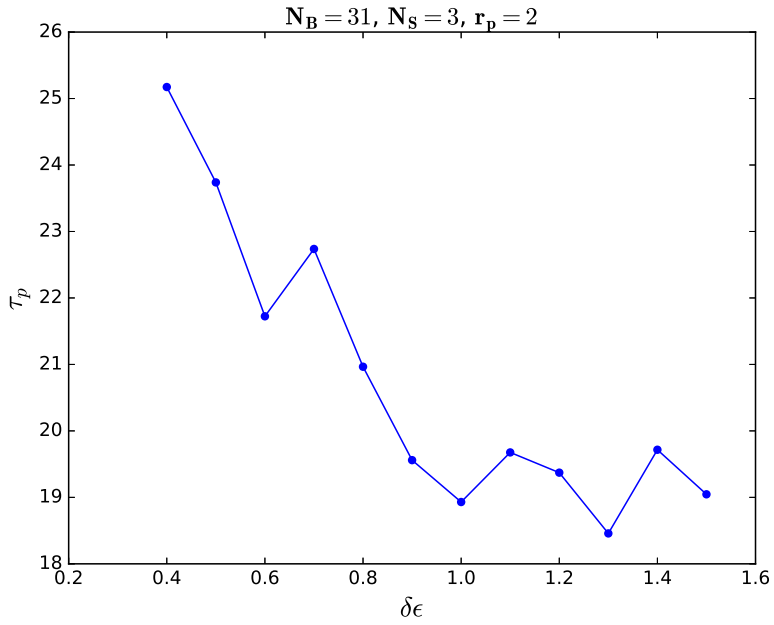

(a) $r_p = 2$

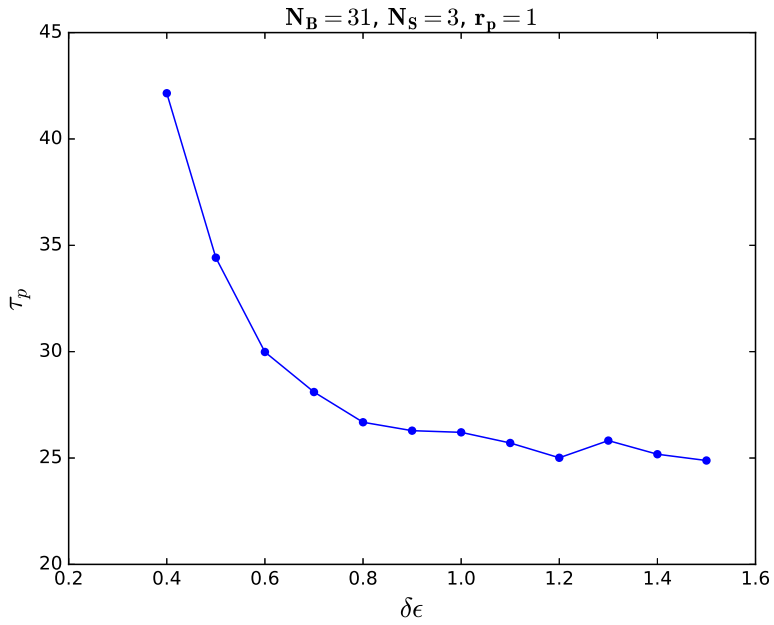

(b) $r_p = 1$

Figure 4.4: Dependence of the most probable PT time τ_p on the field strength $\delta\epsilon$

only a single file translocation is allowed. This may be somehow connected to the peculiar trait of the pore size $r_p = 1.5$ in the field strength dependence of the translocation dynamics.

Figure 4.3 shows the distribution of $\tau/\langle\tau\rangle$ for two different pore sizes, $r_p = 2$ and $r_p = 1$. Several comparisons can be made between the two sub-figures. First, all the curves in the sub-figure 4.3b have a single peak. For the curves in the sub-figure 4.3a, this is not true. This is because only a single file translocation is possible through a pore of size $r_p = 1$. Through wider pores, besides the extended configuration of the polymer, several folded configurations also compete for translocation. The existence of several peaks on some of the curves in the sub-figure 4.3a is due to the characteristic dynamics of these modes of translocations.

Second, it is interesting to note that the rightmost curves in both sub-figures correspond to $\delta\epsilon_c$ for each pore size. The curves in the sub-figure 4.3a are very close together and to $\tau/\langle\tau\rangle$=1 in comparison to those in the other sub-figure. The most probable PT time τ_p and the mean PT time $\langle\tau\rangle$ have different values if the peaks of the curves in the distribution of $\tau/\langle\tau\rangle$ do not lie on the line $\tau/\langle\tau\rangle$=1. In both sub-figures, one can see that the differences between τ_p and $\langle\tau\rangle$ get more significant as $|\delta\epsilon - \delta\epsilon_c|$ increases.

Finally, we see the field strength dependence of the most probable PT time τ_p. Figure 4.4 depicts such relationship for the pore sizes $r_p = 2$ and $r_p = 1$. For the pore size $r_p = 1$, we see a very simple curve indicating that τ_p decreases rapidly, at first, as the field strength increases. The decrease then rapidly vanishes and τ_p stops changing at all for further increases in the field strength. The general trend of the curve for the pore size $r_p = 2$ is the same as that of the curve for the pore size $r_p = 1$; but the trend is disturbed at several positions on the curve for $r_p = 2$. This is due to the existence of multiple modes of translocation for the pore size $r_p = 2$.

4.2 The dependence of the PT time τ on the pore size r_p

In this section, we investigate the effect of the pore size on the translocation dynamics of a comb polymer. We considered pore sizes as wide as $r_p = 6$ and side chain lengths of the comb polymer as long as $N_S = 10$. We felt that side chain lengths are more involved with the effects of the pore size to the translocation dynamics than backbone

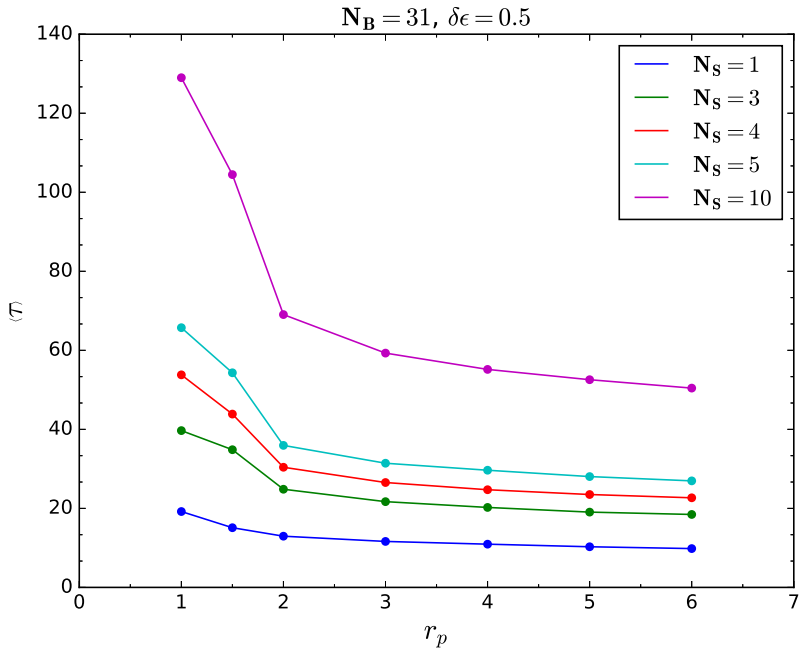

Figure 4.5: Dependence of the mean PT time on the pore radius for a range of side-chain lengths $N_S = 1, 3, 4, 5, 10$

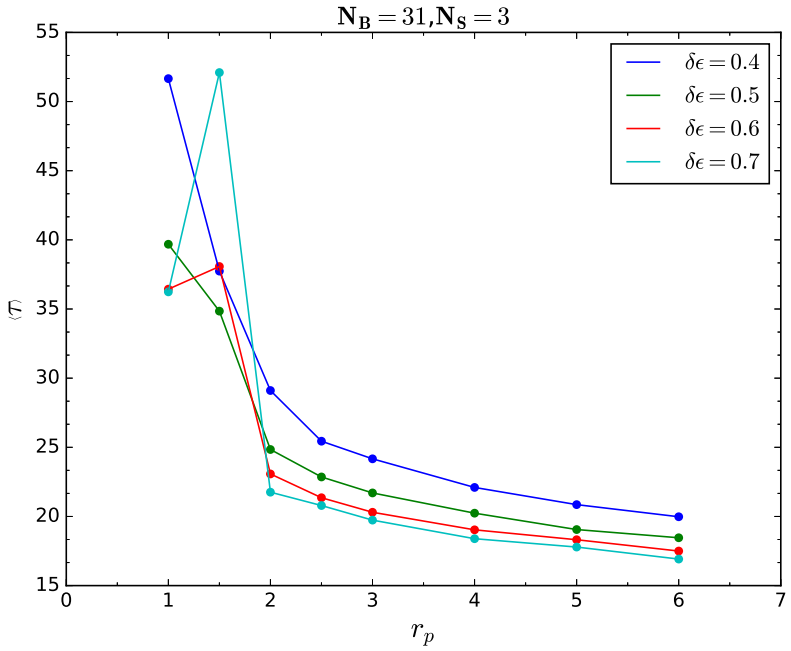

Figure 4.6: Dependence of the mean PT time on the pore radius for four electric field strength values: $\delta\epsilon = 0.4, 0.5, 0.6, 0.7$.

lengths are. So, little attention was given to the backbone lengths of the comb polymer in this subsection.

Figure 4.5 shows the values of the mean PT time $\langle\tau\rangle$ of comb polymers with different side chain lengths, as the radii of the pore vary. The curves in the figure have many features in common. One is that they are all decreasing. This is understandable since the pore-monomer and the monomer-monomer interaction at the pore entrance becomes less and less intense as the pore size increases. If we look more closely, all the curves in the figure can be divided into two regions based on the rate of their decrease. For $r_p \geq 2$, they decrease very slowly in comparison to the other half. In the previous section, we noted that, for the pore size $r_p = 1$, only a single file translocation is allowed and that the pore size $r_p = 1.5$ is where a transition is made from multiple modes of translocation to a single file translocation. PT in folded configuration takes a much less time than PT in extended configuration because in folded configuration several segments of the polymer move simultaneously, reducing the PT time by a factor of roughly the number of the segments. We attribute the contrast between the two regions of the curves to the cutoff of the translocation made in folded configuration in the region $r_p < 2$.

When we turn to the effect of the side chain length on the pore size dependence of the PT time, we observe that curves corresponding to long side chains are steeper than those that correspond to short side chains. For any given pore size, we see from the figure that the longer the side chain is, the higher the mean PT time becomes. This is expected because, just as in the effect of narrowing of the pore, the longer the side chain is, the more crowded is the pore entrance and, hence, the more intense are both the monomer-monomer interaction and the pore-monomer interaction at the pore gate. Apparently, there is a cross term associated with the exacerbation of these interactions when we shrink the pore size while making the side chain length longer. So, the PT times of comb polymers with $N_S = 10$ are more affected than those with $N_S = 5$ when the pore size is reduced. This is why the curves corresponding to longer side chains are steeper.

Incidentally, it is curious that, in this simulation, comb polymers with very long side chains are able to translocate through a pore of size small enough that no two linear polymers can translocate through side by side. This has to do with the flexibility of the polymers since it would be physically impossible for comb polymers with $N_S > 1$ to

squeeze through a pore of size $r_p = 1$ in this simulation if the opposite were true.

Before we conclude this section, we see the effect of the field strength on the pore size dependence of the PT time. Figure 4.6 is prepared to serve this purpose. On a first sight, the curves in the figure look very different from one another. However, if we divide the curves in two regions as before, for the region $r_p \geq 2$, they look very similar to one another. To gain some sense of the apparently chaotic region $r_p < 2$, we need to summon the concept of the critical field strength $\delta\epsilon_c$ developed in the previous region. As we mentioned there, the critical field strength is unique to the pore size if all the other parameters of the translocation are held constant.

According to our simulation result, for the pore size $r_p = 1$, $\delta\epsilon_c$=0.5. For $r_p = 1.5$, $\delta\epsilon_c$=0.4; for $r_p \geq 2$, $\delta\epsilon_c \geq 0.7$. It follows that for all pore sizes, $\delta\epsilon_c \geq 0.4$. So, for the curve corresponding to $\delta\epsilon = 0.4$, no point is associated to field strength above the critical field strength. For the rest of the curves, the same cannot be said. However, for the region $r_p \geq 2$, every point on every curve corresponds to field strength that is no higher than $\delta\epsilon_c$.

Seeing all these together helps one see two regimes of translocation. We name these regimes of translocation as smooth and chaotic. A translocation is said to be in the chaotic regime of translocation if the value of the field strength of the translocation is above the critical value; otherwise, it belongs to the smooth regime of translocation. Now, for the region $r_p \geq 2$ in figure 4.6, every point on every curve is in the smooth regime of translocation. In the other region, some points are in the smooth region while the others are in the chaotic region.

In light of these new concepts, we make two notes. First, for all the curves in figure 4.5 except the curve corresponding to $N_S = 1$, the points at $r_p = 1.5$ lie in the chaotic regime of translocation while all the other points are in the smooth regime. For the curve corresponding to $N_S = 1$, every point is in the smooth regime. A close inspection of the shapes of the curves picks out this curve as being differently shaped from the others at precisely $r_p = 1.5$. Second, figure 4.7 picks out the curves in figure 4.5 and figure 4.6 belonging entirely to the smooth regime of translocation, and displays them separately. Both curves in the figure are very smooth.

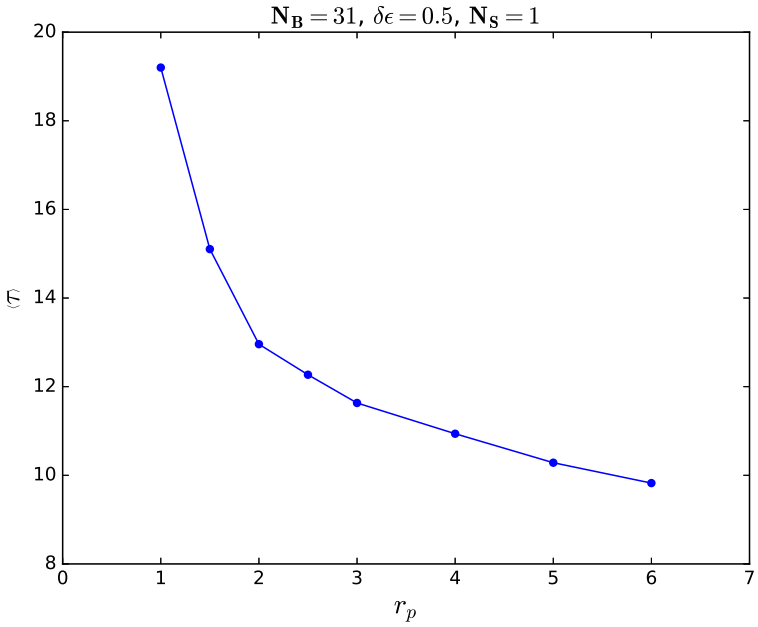

(a)

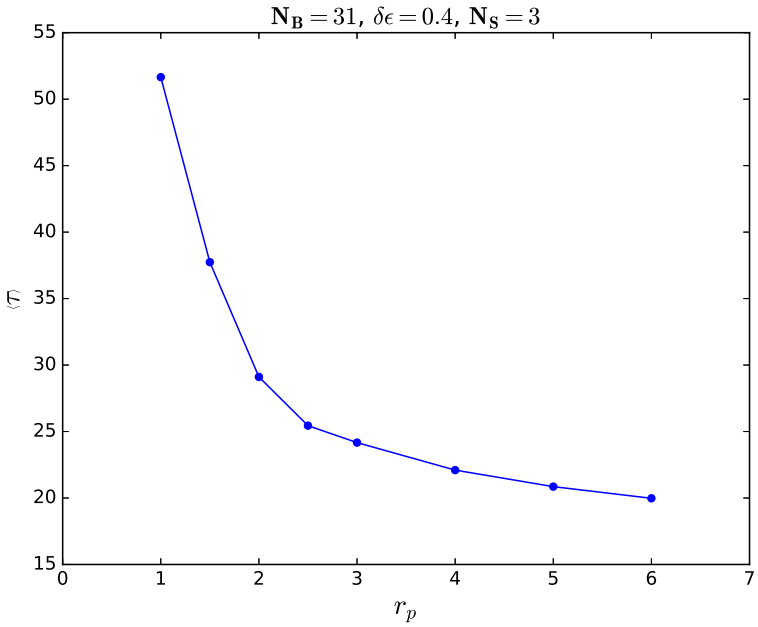

(b)

Figure 4.7: Dependence of the mean PT time $\langle\tau\rangle$ on the pore radius r_p in the regime of smooth translocation

4.3 The dependence of PT time τ on the comb polymer's topology

In the above two sections, we were mainly concerned with the effects of variables exterior to the comb polymer on the polymer's translocation dynamics. Here, we focus on the roles played by the attributes of the comb polymer itself in the context of the translocation dynamics, which we mainly perceive in terms of the PT time τ. These attributes are the backbone length and the side chain length of the comb polymer.

All the results presented in this section are associated with translocations in the smooth regime (see the preceding section).

4.3.1 Backbone length N_B dependence of the mean PT time $\langle\tau\rangle$

In this work, the influence of the backbone length on the translocation dynamics is captured in terms of a power law relationship between the mean PT time and the backbone length, regardless of the pore size, as shown in figure 4.8. In the figure, we can see that the exponent of N_B reduces from 1.72 to 1.30 as the pore radius decreases from $r_p = 4$ to $r_p = 1$. We are more interested in the result associated with the pore $r_p = 1$ since that is where only a single file translocation is made. Figure 4.9 shows the effect of side chain length in the backbone length dependence of the mean PT time for a single file translocation. There, the exponent of N_B reduces from 1.30 to 1.24 as the side chain length decreases from $N_S = 3$ to $N_S = 1$. Since longer side chains are associated to a more intense monomer-monomer and pore-monomer interactions at the pore entrance, it follows that the more intense these interactions are, the greater the value of the exponent of N_B becomes.

The experimentally found exponent of N_B for a linear polymer by Storm *et al.* [20] is 1.30. However, in another experiment done by Chen *et al.*, the reported value of the exponent of N_B is 1 [22]. Also, Wanunu *et al.* reported 1.40 as the value of this exponent based on their experiments [23].

All of the three experimentalists did their translocation experiments with double-stranded DNA molecules. However, the pore sizes they used differ. Wanunu *et al.* preferred pore sizes in the range 2.7-5 nm; Storm *et al.* used a $\sim$10 nm pore while Chen *et al.* used a $\sim$15 nm pore. We mentioned above that great pore-monomer and monomer-

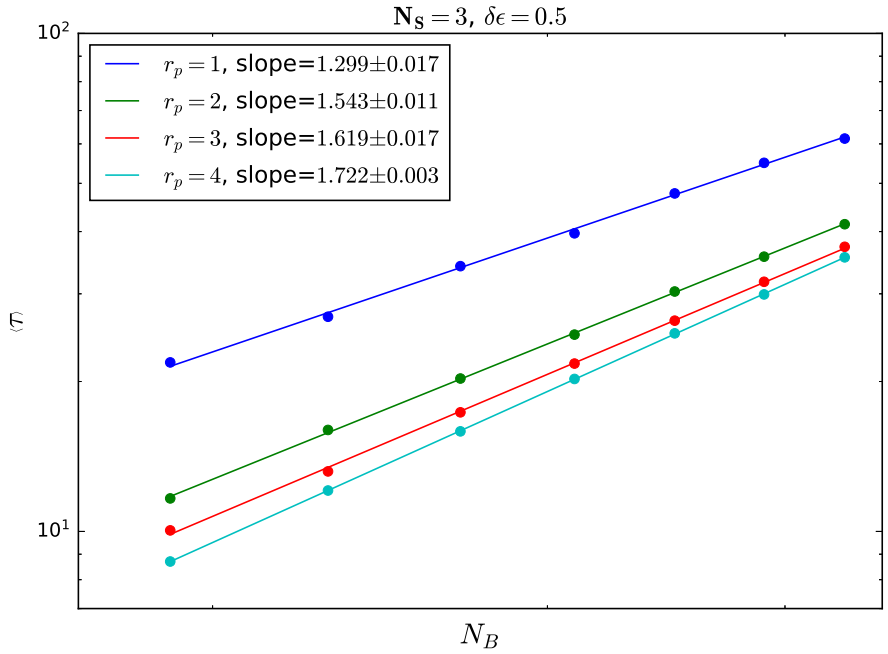

Figure 4.8: Dependence of the mean PT time $\langle\tau\rangle$ on the backbone length N_B for a range of pore sizes $r_p = 1, 2, 3, 4$

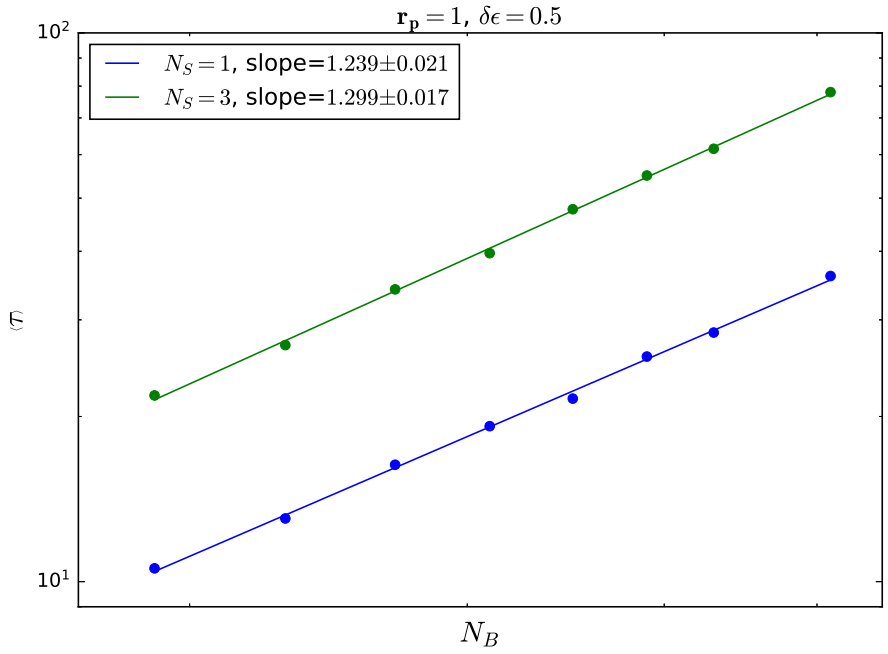

Figure 4.9: Backbone length dependence of the mean PT time $\langle\tau\rangle$ in a single file translocation for the side chain lengths of 1 and 3.

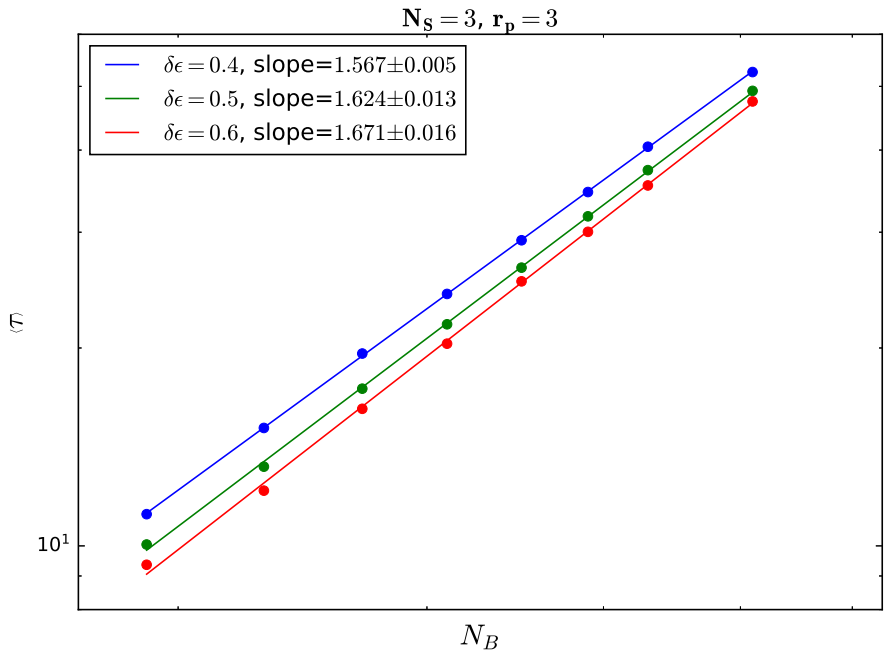

Figure 4.10: Dependence of the mean PT time $\langle\tau\rangle$ on the backbone length N_B for the field strengths $\delta\epsilon = 0.4, 0.5, 0.6$

monomer interactions make the exponent of N_B high. Since narrowing of pores go with worsening of these interactions, the increase of the exponent from 1 to 1.40 as the pore size decreases from ∼15 nm to 2.7-5 nm is quite reasonable.

Next, we briefly see the effect of the field strength on the relationship between the mean PT time and the backbone length. According to figure 4.10, increasing the field strength causes the exponent of N_B to go higher. The validity of this result to only single file translocations has not been tested.

4.3.2 Side chain length N_S dependence of the mean PT time $\langle\tau\rangle$

The study of the dependence of mean PT times on the side chain length does not have a counterpart for linear polymers, unlike that of the mean PT time dependence on the backbone length. So, given that comb polymer translocation studies are very scarce in the literature, the results we are about to present may be brand new. As the figures 4.11 and 4.12 stipulate, the relationship between the side chain length and the mean PT time is linear. From figure 4.11, we see how the pore size affects this linear relationship. The projected value of the graphs at $N_S = 0$ is the mean PT time of a

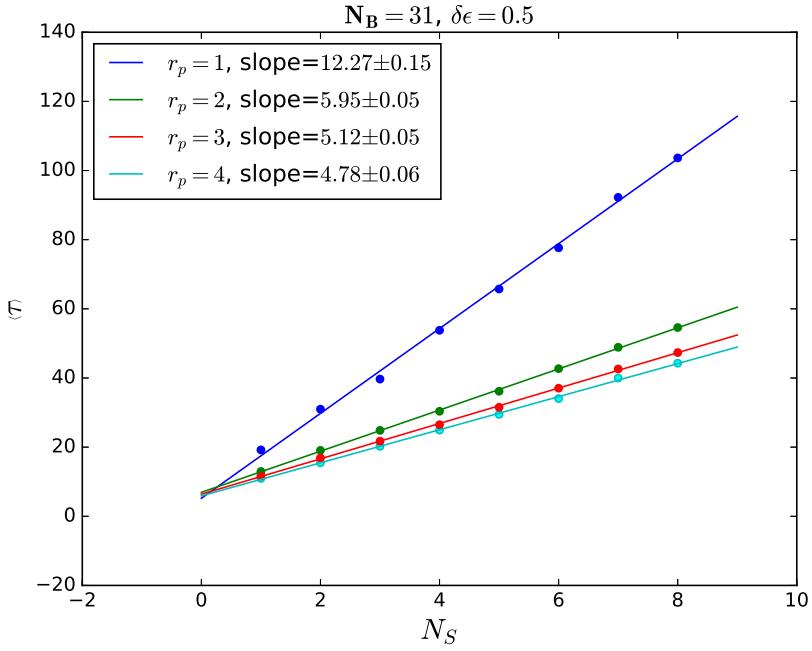

Figure 4.11: Dependence of the mean PT time $\langle\tau\rangle$ on the side chain length N_S for pore sizes that range from $r_p = 1$ to $r_p = 4$

linear polymer. Although the lines in the figure seem to have an intersection at $N_S = 0$, a careful observation contradicts this. As adding a little salt to water enhances its electrical conductivity by a great deal, the tiny differences between the values of the graphs at $N_S = 0$ are magnified when N_S is increased by one. This is a good illustration of the combined effect of side chain length N_S and pore size r_p on the mean PT time $\langle\tau\rangle$. Finally, the exceptionally high value of the slope corresponding to $r_p = 1$ can be attributed to a single file translocation, which is the sole mode of translocation possible through $r_p = 1$.

Figure 4.12 shows the field strength effect on the side chain length dependence of the mean PT time. Here, increasing the field strength decreases the slope of the lines. Again, the validity of this result to a translocation made exclusively in a single file manner has not been checked.

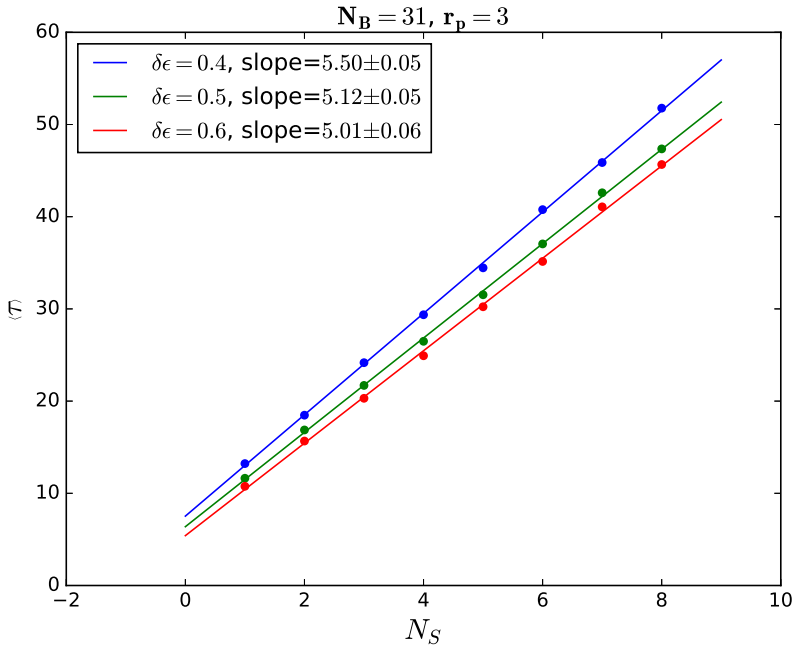

Figure 4.12: Dependence of the mean PT time $\langle\tau\rangle$ on the side chain length N_S for the field strengths $\delta\epsilon = 0.4, 0.5, 0.6$

Chapter 5

Conclusion

The MC study on comb polymer translocation undertaken in this thesis has four translocation variables: the electric field strength, the pore size, and the backbone length and the side chain length of the comb polymer. We found that the electric field strength plays a key role in the translocation dynamics. There is also the role of the pore size. We have seen that the pore size $r_p = 1.5$ is where the transition from multiple modes of translocation to only single file translocation is made. This transition influenced the translocation dynamics in a peculiar way by making the PT particularly sensitive to the field strength.

The influence of the electric field strength on the translocation process can be easily captured from the resultant pattern of the PT time distribution. As the field strength increases from a minimal value, the right-skewed PT time distribution contracts. The narrowest PT time distribution is attained when the electric field strength reaches a critical value $\delta\epsilon_c$. For $\delta\epsilon = \delta\epsilon_c$, the difference between the most probable PT time and the mean PT time is minimum. Further increases in the field strength cause the PT time distribution to spread out.

We have also seen that translocations for field strengths up to $\delta\epsilon_c$ and above $\delta\epsilon_c$ have different properties. For $\delta\epsilon \leq \delta\epsilon_c$, the fraction of stuck polymers in translocation trials is negligible. For $\delta\epsilon > \delta\epsilon_c$, the fraction of stuck polymers increases rapidly as the field strength increases. We identified translocations with $\delta\epsilon \leq \delta\epsilon_c$ as smooth translocations and those with $\delta\epsilon > \delta\epsilon_c$ as chaotic. A collection of translocational measurements is easy to understand if the measurements are categorized as smooth and chaotic, as discussed in section 4.2.

Comb polymers are uniquely suited for the study of pore-polymer interaction due to their side chains. By varying the side chain lengths of comb polymers, we were able to see the effect of the pore-polymer interaction on the dependence of the mean PT time on the backbone length in the first topic of section 4.3. Finally, we discovered a linear relationship between the side chain length and the mean PT time.

Comb polymers are linear polymers with side chains. Therefore, a translocational study on comb polymers benefits greatly from the rich literature on linear polymer translocation. Conversely, the relative topological richness of comb polymers can be used to probe into unresolved issues regarding linear polymer translocation.

Bibliography

[1] M. Rubinstein, R. Colby, Polymer Physics, OUP Oxford, 2003.
URL https://books.google.com.et/books?id=RHksknEQYsYC

[2] M. Doi, Introduction to Polymer Physics, Introduction to Polymer Physics, Clarendon Press, 1996.
URL https://books.google.com.et/books?id=hsjGFLvLnQIC

[3] M. Muthukumar, Entropic barrier theory of polymer translocation, in: Structure and Dynamics of Confined Polymers, Springer, 2002, pp. 227–239.

[4] M. G. Gauthier, Simulation of polymer translocation through small channels: A molecular dynamics study and a new monte carlo approach, Ph.D. thesis, University of Ottawa (Canada) (2008).

[5] J. J. Kasianowicz, E. Brandin, D. Branton, D. W. Deamer, Characterization of individual polynucleotide molecules using a membrane channel, Proceedings of the National Academy of Sciences 93 (24) (1996) 13770–13773.

[6] W. Sung, P. Park, Polymer translocation through a pore in a membrane, Physical review letters 77 (4) (1996) 783.

[7] M. Muthukumar, Polymer translocation through a hole, The Journal of Chemical Physics 111 (22) (1999) 10371–10374.

[8] D. K. Lubensky, D. R. Nelson, Driven polymer translocation through a narrow pore, Biophysical journal 77 (4) (1999) 1824–1838.

[9] J. Chuang, Y. Kantor, M. Kardar, Anomalous dynamics of translocation, Physical Review E 65 (1) (2001) 011802.

[10] Y. Kantor, M. Kardar, Anomalous dynamics of forced translocation, Physical Review E 69 (2) (2004) 021806.

[11] T. Ikonen, A. Bhattacharya, T. Ala-Nissila, W. Sung, Unifying model of driven polymer translocation, Physical Review E 85 (5) (2012) 051803.

[12] M. Muthukumar, Theory of capture rate in polymer translocation, The Journal of chemical physics 132 (19) (2010) 05B605.

[13] T. Sakaue, Nonequilibrium dynamics of polymer translocation and straightening, Physical Review E 76 (2) (2007) 021803.

[14] T. Sakaue, Sucking genes into pores: Insight into driven translocation, Physical Review E 81 (4) (2010) 041808.

[15] A. Milchev, Single-polymer dynamics under constraints: scaling theory and computer experiment, Journal of Physics: Condensed Matter 23 (10) (2011) 103101.

[16] C. T. A. Wong, M. Muthukumar, Polymer translocation through α-hemolysin pore with tunable polymer-pore electrostatic interaction, The Journal of chemical physics 133 (4).

[17] A. Meller, L. Nivon, D. Branton, Voltage-driven dna translocations through a nanopore, Physical Review Letters 86 (15) (2001) 3435.

[18] J. Li, M. Gershow, D. Stein, E. Brandin, J. A. Golovchenko, Dna molecules and configurations in a solid-state nanopore microscope, Nature materials 2 (9) (2003) 611–615.

[19] J. B. Heng, C. Ho, T. Kim, R. Timp, A. Aksimentiev, Y. V. Grinkova, S. Sligar, K. Schulten, G. Timp, Sizing dna using a nanometer-diameter pore, Biophysical journal 87 (4) (2004) 2905–2911.

[20] A. J. Storm, C. Storm, J. Chen, H. Zandbergen, J.-F. Joanny, C. Dekker, Fast dna translocation through a solid-state nanopore, Nano letters 5 (7) (2005) 1193–1197.

[21] A. J. Storm, J. Chen, H. Zandbergen, C. Dekker, Translocation of double-strand dna through a silicon oxide nanopore, Physical review E 71 (5) (2005) 051903.

[22] P. Chen, J. Gu, E. Brandin, Y.-R. Kim, Q. Wang, D. Branton, Probing single dna molecule transport using fabricated nanopores, Nano letters 4 (11) (2004) 2293–2298.

[23] M. Wanunu, J. Sutin, B. McNally, A. Chow, A. Meller, Dna translocation governed by interactions with solid-state nanopores, Biophysical journal 95 (10) (2008) 4716–4725.

[24] C. Wang, S. Sensale, Z. Pan, S. Senapati, H.-C. Chang, Slowing down dna translocation through solid-state nanopores by edge-field leakage, Nature communications 12 (1) (2021) 140.

[25] K. Chen, I. Jou, N. Ermann, M. Muthukumar, U. F. Keyser, N. A. Bell, Dynamics of driven polymer transport through a nanopore, Nature Physics 17 (9) (2021) 1043–1049.

[26] A. Aksimentiev, J. B. Heng, G. Timp, K. Schulten, Microscopic kinetics of dna translocation through synthetic nanopores, Biophysical journal 87 (3) (2004) 2086–2097.

[27] M. Muthukumar, C. Kong, Simulation of polymer translocation through protein channels, Proceedings of the National Academy of Sciences 103 (14) (2006) 5273–5278.

[28] K. Luo, I. Huopaniemi, T. Ala-Nissila, S.-C. Ying, Polymer translocation through a nanopore under an applied external field, The Journal of chemical physics 124 (11).

[29] S.-S. Chern, A. E. Cárdenas, R. D. Coalson, Three-dimensional dynamic monte carlo simulations of driven polymer transport through a hole in a wall, The Journal of Chemical Physics 115 (16) (2001) 7772–7782.

[30] C. Forrey, M. Muthukumar, Langevin dynamics simulations of ds-dna translocation through synthetic nanopores, The Journal of chemical physics 127 (1).

[31] A. Izmitli, D. C. Schwartz, M. D. Graham, J. J. de Pablo, The effect of hydrodynamic interactions on the dynamics of dna translocation through pores, The Journal of chemical physics 128 (8).

[32] K. Luo, T. Ala-Nissila, S.-C. Ying, Polymer translocation through a nanopore: A two-dimensional monte carlo study, The Journal of chemical physics 124 (3).

[33] K. Luo, S. T. Ollila, I. Huopaniemi, T. Ala-Nissila, P. Pomorski, M. Karttunen, S.-C. Ying, A. Bhattacharya, Dynamical scaling exponents for polymer translocation through a nanopore, Physical Review E 78 (5) (2008) 050901.

[34] K. Luo, T. Ala-Nissila, S.-C. Ying, A. Bhattacharya, Heteropolymer translocation through nanopores, The Journal of chemical physics 126 (14).

[35] M. Tilahun, Y. B. Tatek, End-pulled translocation of a star polymer out of a confining cylindrical cavity, Macromolecular Theory and Simulations 30 (2) (2021) 2000090.

[36] M. Tilahun, Y. B. Tatek, Star-shaped polymer translocation into a nanochannel: Langevin dynamics simulations, Physica Scripta 98 (2) (2023) 025006.

[37] L. Song, M. R. Hobaugh, C. Shustak, S. Cheley, H. Bayley, J. E. Gouaux, Structure of staphylococcal α-hemolysin, a heptameric transmembrane pore, Science 274 (5294) (1996) 1859–1865.

[38] V. V. Palyulin, T. Ala-Nissila, R. Metzler, Polymer translocation: the first two decades and the recent diversification, Soft matter 10 (45) (2014) 9016–9037.

[39] D. Panja, G. T. Barkema, A. B. Kolomeisky, Through the eye of the needle: recent advances in understanding biopolymer translocation, Journal of Physics: Condensed Matter 25 (41) (2013) 413101.

[40] J. Li, D. Stein, C. McMullan, D. Branton, M. J. Aziz, J. A. Golovchenko, Ion-beam sculpting at nanometre length scales, Nature 412 (6843) (2001) 166–169.

[41] A. Storm, J. Chen, X. Ling, H. Zandbergen, C. Dekker, Fabrication of solid-state nanopores with single-nanometre precision, Nature materials 2 (8) (2003) 537–540.

[42] D. Branton, D. W. Deamer, A. Marziali, H. Bayley, S. A. Benner, T. Butler, M. Di Ventra, S. Garaj, A. Hibbs, X. Huang, et al., The potential and challenges of nanopore sequencing, Nature biotechnology 26 (10) (2008) 1146–1153.

[43] D. W. Deamer, D. Branton, Characterization of nucleic acids by nanopore analysis, Accounts of chemical research 35 (10) (2002) 817–825.

[44] M. Muthukumar, Polymer translocation, CRC press, 2016.

[45] S. Buyukdagli, J. Sarabadani, T. Ala-Nissila, Theoretical modeling of polymer translocation: From the electrohydrodynamics of short polymers to the fluctuating long polymers, Polymers 11 (1) (2019) 118.

[46] I. Carmesin, K. Kremer, The bond fluctuation method: a new effective algorithm for the dynamics of polymers in all spatial dimensions, Macromolecules 21 (9) (1988) 2819–2823.

Declaration

This thesis is my original work and has not been presented for a degree in any other university.

All the sources of material used for the thesis have been duly acknowledged.

Bruh Tesfa

January, 2024